

Determination of Propagation Rate Coefficients for Methyl and 2-Ethylhexyl Acrylate via High Frequency PLP–SEC under Consideration of the Impact of Chain Branching

Thomas Junkers,^{*,†,‡} Maria Schneider-Baumann,[†] Sandy S. P. Koo,[†] Patrice Castignolles,[§] and Christopher Barner-Kowollik^{*,†}

[†]Preparative Macromolecular Chemistry, Karlsruhe Institute of Technology (KIT), Institut für Technische Chemie und Polymerchemie, Engesserstr. 18, 76128 Karlsruhe, Germany, [‡]Universiteit Hasselt, Institute for Materials Research, Agoralaan, Gebouw D, B-3590 Diepenbeek, Belgium, and [§]School of Natural Science, Australian Centre for Research on Separation Science, University of Western Sydney, Locked Bag 1797, Penrith South DC, NSW 1797, Australia

Received September 14, 2010; Revised Manuscript Received November 8, 2010

ABSTRACT: The radical propagation rate coefficients, k_p , of methyl acrylate (MA) and 2-ethylhexyl acrylate (EHA) have been determined in bulk via high frequency (500 Hz) pulsed laser polymerization coupled to size exclusion chromatography (PLP–SEC) up to elevated temperatures ($20 \leq T/^\circ\text{C} \leq 80$). Prior to the analysis of the generated polymeric material, an investigation into the branching behavior of the generated polymers has been undertaken, employing the concept of local dispersity, $D(V_e)$. In addition, the Mark-Houwink-Kuhn-Sakurada parameters for both poly(MA) and polyEHA were determined at each studied reaction temperature. The temperature averaged values read ($K = 10.2 \times 10^{-5} \text{ dL g}^{-1}$; $\alpha = 0.741$) and ($K = 9.85 \times 10^{-5} \text{ dL g}^{-1}$; $\alpha = 0.719$) for poly(MA) and polyEHA, respectively. The local dispersity data indicate that branching in polyEHA may be considerably more prevalent than in poly(MA), as with increasing temperature polymer microinhomogeneities are observed. Consequently, the Arrhenius parameters for k_p of EHA are beset with a larger error than those of MA. The activation parameters in the temperature range between 20 and 80 °C read: $E_A^{\text{MA}} = 18.5 (+0.8 \text{ to } -0.9) \text{ kJ} \cdot \text{mol}^{-1}$ and $A^{\text{MA}} = 2.5 (+1.2 \text{ to } -0.6) \times 10^7 \text{ L} \cdot \text{mol}^{-1} \cdot \text{s}^{-1}$; $E_A^{\text{EHA}} = 15.8 (+1.6 \text{ to } -1.4) \text{ kJ} \cdot \text{mol}^{-1}$ and $A^{\text{EHA}} = 9.1 (+10.1 \text{ to } -2.9) \times 10^6 \text{ L} \cdot \text{mol}^{-1} \cdot \text{s}^{-1}$.

Introduction

Despite the advanced level of new developments in the field of synthetic polymer chemistry, there is today still demand for precise and accurate rate coefficients of the individual reactions occurring in free-radical polymerizations. Without knowledge of such parameters, the design of novel processes and the refinement of existing techniques is hampered. In particular, the kinetic modeling of reactions on laboratory or large scale reactors relies mostly on the availability of correct and reliable kinetic rate coefficients. With advanced polymerization systems such as atom transfer radical polymerization, ATRP,¹ reversible addition–fragmentation chain transfer polymerization, RAFT,² or nitroxide-mediated polymerization, NMP,³ the focus is often on the specific questions that arise from the specific control mechanism, yet in many cases even the fundamental coefficients of initiation, propagation, and termination are only known with limited accuracy.^{4,5}

The rate coefficient to which the most direct access is available by modern laser polymerization methods is the propagation rate coefficient, k_p . This coefficient can be determined via analysis of the typical molecular weight pattern that is generated upon sequential initiation and termination of growing chains caused by irradiation with a pulsed laser. The pulsed laser polymerization–size exclusion chromatography technique, PLP–SEC (for details regarding the technique see below)—developed in

the late 1980s⁶—has proven to be very reliable as the accuracy of the method is virtually only limited by the accuracy of the determination of molecular weights.⁷ Indeed, a large number of data was provided in the past 20 years for a multitude of radically polymerizable monomers; for selected monomers, an IUPAC working party has collated benchmark values so that standardized values have become available, including for *n*-butyl acrylate.⁸ For the academically and industrially important class of acrylate monomers, only few data are available, a fact that was also noted by the IUPAC working party. The lack of wide ranging data is due to two intrinsic problems that are associated with acrylates. One is the general failure of the PLP–SEC experiment at elevated temperatures due to significant side reactions. The other problem is the accurate determination of molecular weight distributions via standard size exclusion chromatography (SEC). Both have their origin in the formation of so-called midchain radicals during the polymerization process.^{9–13} Thereby, the radical center at the growing chain end (which is of secondary nature) is transformed into a tertiary radical by a proton shift reaction or transfer to polymer, respectively. These transfer reactions can occur via different pathways, either *inter*- or *intramolecularly*. Midchain radicals, MCR, can undergo a multitude of reactions, namely addition to monomer (at a largely reduced reaction rate), termination or β -scission. The MRC location on the polymer backbone where the radical is transferred to is generally random, with the exception of the [1,5] H-shift that is occurring via a favored six-membered ring structure, in which case the reaction is referred to as backbiting. The exact mechanisms and the implications that follow from these reactions have been described in detail and thus are not reiterated here.^{8,10,12–14} A detailed overview over the

*Corresponding authors. (T.J.) E-mail: thomas.junkers@uhasselt.be. Telephone: +32 (11) 26 8318. Fax: +32 (11) 26 8399. (C.B.-K.) E-mail: christopher.barner-kowollik@kit.edu, Telephone: +49 721 608 5641. Fax: +49 721 608 5740.

consequences of transfer to polymer can be found here¹⁴ and in the references cited therein. For the purposes of the current study, it is sufficient to note that from the different mechanisms either short chain branches are formed in the residual polymer from backbiting or long chain branches from random transfer. Additionally, a general retardation occurs due to the relatively high stability of the MCRs before they undergo further addition of monomer units. On the basis of the above background, the inherent problems in acrylate PLP–SEC can be understood: The retardation of the reaction leads to a loss of the time-chain-length correlation¹³ on which the PLP–SEC technique is based. Concomitantly, the branching itself leads to incorrect calibrations of an SEC apparatus. Hamielec predicted this as branched polymers behave differently from their linear counterparts with respect to their hydrodynamic volume and therefore elution volume on a chromatography column.^{15–17} Our experimental investigations have confirmed the effect to be significant.^{18–21}

The problem of chain growth retardation can largely be overcome by employing fast pulse rates.^{22,23} With the usage of a 500 Hz excimer laser, k_p for *n*-butyl acrylate became available for temperatures exceeding 70 °C, whereas with the older 100 Hz systems, only data up to ambient temperature could be collated⁸ (transfer to polymer reactions are associated with a higher activation energy than propagation, thus the disturbing influences of these reactions are not as severe at lower temperatures). The k_p s obtained with the 500 Hz laser system are in excellent agreement with the low-temperature data that were collated by the IUPAC. Since then we have investigated various acrylate monomers^{24,25} as well as acrylonitrile²⁶ and vinyl acetate²⁷ with the high-frequency laser setup.

In the current contribution we aim to fill an existing gap and provide accurate propagation rate coefficient data for the monomers methyl acrylate, MA, and 2-ethylhexyl acrylate, EHA. Both monomers are extensively employed in polymer design and only insufficient propagation rate data is available to date,⁴ even though MA is probably the best studied acrylate monomer after *n*-butyl acrylate with regard to its polymerization kinetics. As noted above, SEC of polyacrylates is far from simple and problems in the accurate determination of molecular weights have been observed including polyEHA²¹ and polyMA.²⁰ Before presenting the results from PLP for the two monomers, we will therefore discuss the separation of polyMA and polyEHA in SEC in detail to arrive at a as reliable as possible determination of molecular weights and at an error estimate for obtained data. In this context, we employ the concept of local dispersity, i.e. the instantaneous dispersity of polymers at a given elution volume.¹⁸ Local dispersities above one are a signature for problems in determination of molecular weights,^{18,20} and preliminary observations have shown that this concept is useful for the evaluation of PLP data of acrylates.²¹

Experimental Part

Materials. Methyl acrylate (MA, VWR, 99%), 2-ethylhexyl acrylate (EHA, Acros, 99%), 2,2-dimethoxy-2-phenylacetophenone (DMPA, Aldrich, 99%), and toluene (Scharlau, HPLC grade) were used as received. Hydroquinone (Aldrich), methanol (VWR), and tetrahydrofuran (Scharlau, HPLC grade) were all used as received.

Pulsed Laser Polymerization Experiments. Bulk monomer solutions containing 5×10^{-3} mol L⁻¹ 2,2-dimethoxy-2-phenylacetophenone (photoinitiator) were transferred into sample vials (containing close to 0.4 mL of reaction solution each) which were sealed with rubber septa. Oxygen was removed by purging the samples with nitrogen for approximately 2 min. The sample vial was subsequently placed into a stainless steel sample holder that was brought to the required temperature by a thermostat (VWR 1196D). The temperature was measured directly at the sample. The samples were allowed to equilibrate

at the reaction temperature for close to 5 min and subsequently initiated by laser pulsing. Laser initiation was achieved by a Coherent Xantos XS-500 excimer laser operated at the XeF-line of 351 nm. The laser beam, which was adjusted to an energy of close to 2.5 mJ/pulse hitting the sample, was redirected to illuminate the vial from the bottom. High repetition laser pulsing might induce a temperature increase. Measurement of the temperature in the sample was carried out in a previous study²² and an average increase of less than 1 °C was observed. A temperature increase due to imperfect heat dissipation is thus negligible. After polymerization, a hydroquinone/methanol solution was added to the samples which are then left for evaporation of the solvent and monomer. Monomer conversion was determined gravimetrically.

Characterization. For the determination of molecular weight distributions (MWD) obtained from PLP, a Varian system comprising an auto injector, a Polymer Laboratories 5.0 μ m bead-size guard column, followed by three linear PL columns (PLgel 5 μ m MIXED-C) and a differential refractive index detector using THF as the eluent at 40 °C with a flow rate of 1 mL·min⁻¹ was used. The SEC system was calibrated using narrow polystyrene and poly(methyl methacrylate) standards (PSS) ranging from 160 to 6×10^6 g mol⁻¹. The resulting molecular weight distributions have been recalibrated employing the specific Mark–Houwink–Kuhn–Sakurada parameters of the corresponding polymer, for polystyrene ($K = 14.1 \times 10^{-5}$ dL·g⁻¹ and $\alpha = 0.70$)²⁸ and poly(methyl methacrylate) ($K = 12.8 \times 10^{-5}$ dL·g⁻¹ and $\alpha = 0.69$).²⁹

The triple-detection chromatographic setup used for the determination of local dispersities and MHKS parameters consisted of a modular system (Polymer Standard Service, PSS, Mainz/Agilent 1200 series) incorporating an ETA2010 viscometer (WGE Dr. Bures) and a light-scattering unit (PSS SLD7000/BI- M_w A, Brookhaven Instruments). Sample separation is achieved via two linear columns provided by PSS (SDV-Lux-1000 Å and 10^5 Å, 5 μ m) with THF as the eluent at 35 °C with a flow rate of 1 mL·min⁻¹. The system was calibrated using polystyrene standards (PSS, see above). The employed triple detection column system features a lower resolution and thus the molecular weight distributions—although being prepared via PLP experiments—employed to derive the local dispersities, do not feature a PLP distribution. The refractive index increment dn/dc , where n is the refractive index and c is polymer concentration, employed in calculation of the molecular weights read for polyMA $dn/dc = 0.068$ mL·mg⁻¹,³⁰ and for poly(2-EHA) $dn/dc = 0.070$ mL·mg⁻¹.³¹ It should be noted that dn/dc is associated with some uncertainty and slightly different values from the ones given can be found in the literature.^{19,20} The discrepancy is however small and close analysis of the data shows that only minor changes in the resulting molecular weights and dispersities are obtained when other values for dn/dc are used.

For data treatment, the raw data are corrected for the interdetector delay using WinGPC before $D(V_e)$ is actually calculated. As is commonly carried out for branched polymers, the light scattering raw data were fitted according to Berry.³² The obtained $\bar{M}_w(V_e)$ are then smoothed to remove noise from the signal using Origin software. The Universal calibration curve from refractometer-viscometer SEC is fitted using a fifth order polynomial function. The data from the viscometer are directly processed without applying any smoothing procedure as the scatter of the residual plots were sufficiently low throughout the whole study. The $\bar{M}_w(V_e)$ and $\bar{M}_n(V_e)$ curves were not fitted, since it often results in mathematical artifacts when constructing the dispersity plot.

Results and Discussion

The Local Dispersity of Poly(methyl acrylate) and Poly(2-ethylhexyl acrylate) Determined via SEC. As branched

polymers have a different hydrodynamic volume compared to linear polymer chains and thus different retention times on a SEC column, the material that is eluted at any given time is structurally not homogeneous but consists of a distribution of polymers with the individual sizes depending on the degrees of branching. The conventional calibration of SEC thus must in principle fail if the material shows inhomogeneous branching; the Mark–Houwink–Kuhn–Sakurada MHKS relation that correlates the molecular weight M of a polymer with its intrinsic viscosity $[\eta]$ (and hence also its hydrodynamic volume HV) via the parameters K and α can no longer be used for universal calibration, because the MHKS relation $[\eta] = K \cdot M^\alpha$ is only strictly valid for polymers with identical chain architecture, and thus the parameters may vary if chain branching occurs.

The number of branches in a polyacrylate increases with temperature as expected from semiquantitative studies,³³ and recently demonstrated by precise and accurate melt-state NMR measurements.^{20,34} The rate of backbiting (and most likely also of random transfer) increases rapidly with temperature,³⁵ and at 60 °C already over 2% of branches (per polymerized monomer unit) in the polymer can be found, as has been shown, e.g., for poly(*n*-butyl acrylate).³⁴ The occurrence of branching thus poses a severe problem for the analysis of polyacrylate samples via conventional SEC as the exact branching distribution in the samples is unknown: neither for the individual length of branches nor in relation to overall molecular weight. In particular, long chain branches that are formed upon random transfer to polymer events were found to have a profound effect on the molecular weight distribution.^{18,21} Long-chain branched polymers have a smaller hydrodynamic volume compared to short-chain branched or strictly linear polymers at a given molecular weight. Thus, at different elution volumes, a mixture of linear, short-chain branched and long-chain branched polymers will elute that are not identical in molecular weight, with the exact difference being unknown.¹⁹ Such a variety of chain architectures will undoubtedly affect the molecular weight distribution analysis, especially with respect to the determination of the inflection points, which need to be determined for arriving at propagation rate coefficients via the PLP–SEC technique. To address the above problem and to provide a method for other researchers to analyze polyacrylate based samples, we present a procedure that first characterizes the polymer samples with respect to their branching homogeneity. To achieve the above aim, the so-called local dispersity $D(V_e)$ of the sample at any given elution volume was determined. Local dispersity is a concept introduced by Hamielec for branched poly(vinyl acetate). For each elution volume element, V_e , the local number-average molecular weights, $\overline{M}_n(V_e)$, can be determined via viscometry in conjunction with universal calibration data treatment. At the same time, local weight-average molecular weights, $\overline{M}_w(V_e)$, are accessible via a light scattering detector. The ratio $\overline{M}_w(V_e)/\overline{M}_n(V_e)$ is subsequently defined as the local dispersity, $D(V_e)$. This definition is analogous to the concept of dispersity of a polymer, yet the local dispersity is calculated for each elution volume element instead for the entire chromatogram. If homogeneous material is eluted on the SEC system, $D(V_e) = 1$ is obtained as both viscometry and light scattering result in the same molecular weight (assuming that the separation on the column is almost perfect and indeed monodisperse material is eluted).¹⁹ Is the sample branched, however, then different molecular weights elute as described above. Thus, the number and the weight-average molecular weight differ, resulting in a local dispersity exceeding unity.¹⁸ Thus, $D(V_e)$ can be employed as

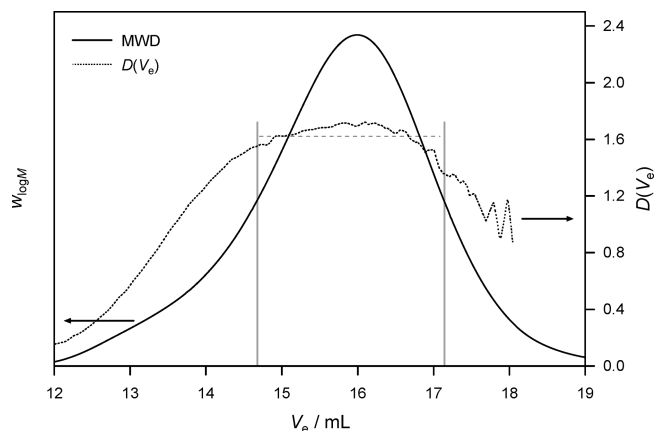


Figure 1. Plot of $D(V_e)$ for a PLP sample produced at 71 °C in comparison to the RI detector signal of the same sample. The gray vertical lines indicate the limits (half height of the chromatogram) in which the average $D(V_e)$ (dashed line) is deduced.

Table 1. Average Local Dispersities of Polyacrylate Samples Made via PLP at Different Reaction Temperatures

poly(methyl acrylate)		poly(2-ethylhexyl acrylate)	
$T/^\circ\text{C}$	$\bar{D}(V_e)$	$T/^\circ\text{C}$	$\bar{D}(V_e)$
19.8	1.20	10.1	0.95
29.9	1.17	20.0	1.31
40.3	1.30	29.7	1.14
50.2	1.09	40.8	1.42
60.6	1.08	50.8	1.52
70.0	1.15	60.9	1.43
81.2	1.18	71.2	1.64
		81.2	1.96

a quantitative measure for the level of branching in a sample, even if the number of branches itself cannot be estimated from it. As proposed before,²¹ the local dispersity can also be employed to estimate the error from conventional SEC analysis by assuming that the “true” molecular weight lies within the local molecular weight distribution, whose broadness is given by the local dispersity, i.e., $\overline{M}_w(V_e)$ and $\overline{M}_n(V_e)$. Thus, for a $D(V_e)$ of for example 1.2, a error of the molecular weight determination of 20% can be envisaged.

A plot of $D(V_e)$ for a PLP sample made from EHA at 71 °C is shown as an example in Figure 1. The $D(V_e)$ plot is superimposed with the RI detector signal to allow for an estimation of the polymer concentration at the given elution volumes.

As can be observed from Figure 1, the local dispersity changes with the elution volume, but goes through a plateau value at elution volumes where most of the polymer is eluted. Such behavior is not seen for all samples, but for many. $D(V_e)$ plots for all analyzed samples can be found in the Supporting Information. The lower local dispersities at the shoulder of the distribution does not necessarily reflect a better homogeneity of the samples. It may just be a consequence of the lower signal-to-noise ratio of both the viscosimeter and the light-scattering detector and thus a largely reduced sensitivity.³⁶ Therefore, to quantify $D(V_e)$ for polymers made a different reaction temperatures, the average dispersity is taken at half the height of the elugram (RI signal), and $D(V_e)$ is determined as the mean value falling in this region. The resulting average values are collated in Table 1 and visualized in Figure 2.

It is important to note that although in Figure 2 a linear fit of the data has been carried out, this fit should be considered an aide to guide the eye to discern trends in the data rather

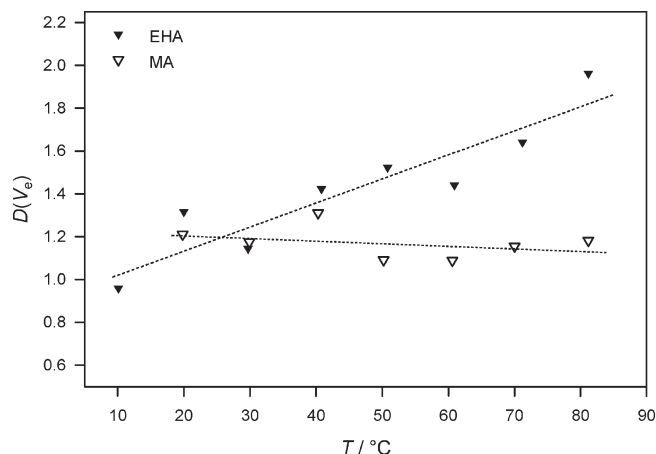


Figure 2. Average local dispersities of polyacrylate samples made via PLP at different reaction temperatures.

than as a statement that a linear relationship between $D(V_c)$ and temperature for either polyEHA or poly(MA) exists. Nevertheless, trends can clearly be observed. At first glance—surprisingly—almost no dependence of the local dispersity on temperature is seen in the poly(MA) samples. Between 20 and 80 °C all data scatter around $D(V_c) = 1.2$ indicating a relatively high consistency of the heterogeneity of the polymer samples. This should, however, not be interpreted in the way that predominantly linear chains are formed; a consistency can also indicate a relatively evenly distributed amount of chain branches. Thus, larger $D(V_c)$ do not necessarily indicate a higher degree of branching. A similar effect has been observed before for poly(*n*-butyl acrylate) and it was concluded that for *n*-butyl acrylate mostly short-chain branched material is formed under some PLP conditions that is, however, relatively homogeneous. It is known that methyl acrylate features a very similar propensity toward midchain radical formation compared to *n*-butyl acrylate under PLP conditions as was determined via ESR spectroscopy.³⁷ Thus, a similar conclusion as for *n*-butyl acrylate may be drawn for MA, i.e. the formation of mainly short chain branches, with limited heterogeneity in SEC due to branching.

A different situation is seen for polyEHA: While at low reaction temperatures (10 °C), a local dispersity of virtually unity is seen—and thus an ideal case of chain separation—a strong increase of $D(V_c)$ with reaction temperature is observed; at 80 °C, $D(V_c)$ is already as high as 2. High local dispersities were indeed observed for polyEHA before.²¹ No data on the rate of backbiting or the accumulated amount of MCRs under PLP conditions are available for this monomer. The degree of branching has been measured by ¹³C NMR for poly(*n*-butyl acrylate)³⁸ and polyEHA³⁹ obtained by identical conventional radical polymerization processes and the one of polyEHA is significantly higher but close to the one of poly(*n*-butyl acrylate).²⁰ Furthermore, EHA polymerization behaves similarly to other acrylates in terms of macromonomer formation.⁴⁰ It can thus be assumed, that EHA also undergoes extensive transfer to polymer reactions in a similar fashion to other acrylates under almost identical reaction conditions.⁴¹ If the rate of backbiting (or β -scission, respectively) would be very different from the other acrylate monomers, the same product (macromonomers) would not be formed. A possible explanation for the large difference in behavior with respect to the local dispersity between MA and EHA can be given if one assumes that EHA undergoes significantly more long-chain

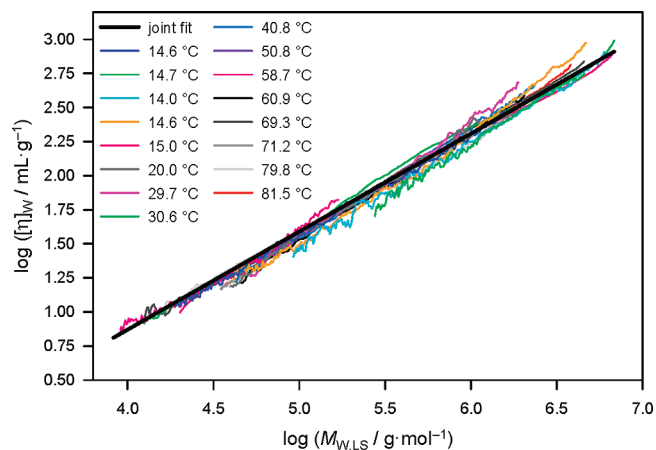


Figure 3. Linear regions of intrinsic viscosity for polyEHA from which MHKS parameters were determined. The linear black line represents the best fit of all data presented in the figure. The temperature under which the individual polyEHA samples were generated are found in the legend.

branching than short-chain branching. Long chain-branches have a more profound effect on the hydrodynamic volume of a polymer coil thus increasing the size-disparity at a given elution volume. It may be hypothesized that EHA, by virtue of its relatively bulky ester side chain, hinders the formation of a six-membered ring transition structure that is often suggested for the backbiting reaction, leading to more random transfer events. However, regardless of the reason for the larger $D(V_c)$ values, an increased uncertainty in molecular weight distribution must be envisaged for EHA.

After the polymer samples were analyzed with respect to branching, a further step that needs to be taken to allow for a comprehensive molecular weight analysis via conventional SEC is the determination of MHKS parameters. Because of the varying degrees of branching, especially with polyEHA, a change in the observable MHKS parameters with changing reaction conditions must be taken into account as a worst case scenario. The same data that have been used to derive the local dispersity plots can also be used to determine the MHKS relation for each sample by directly plotting the measured intrinsic viscosity $[\eta]$ vs the molecular weight as determined by the light scattering detector. In Figure 3, overlaps of the MHKS plots for PLP samples of polyEHA generated under various reaction conditions are depicted. According data are given for poly(MA) in Figure 4. As constant $D(V_c)$ was seen with poly(MA), more samples have been analyzed for polyEHA.

Within the experimental scatter, no trend can be seen with changing reaction temperature for polyEHA. The combined data can in fact be represented by a joint linear fit (that is represented by the thick black line). The MHKS parameters (Table 2) significantly differ from the ones obtained for linear polyEHA.^{20,42,43} Inspection of Figure 4 suggest the conclusion that even though apparently an increased branching heterogeneity exist within the polyEHA samples (see Figure 2), the MHKS relation can still be used as fitting parameter. Such a finding is quite serendipitous as it allows one to analyze all polyEHA samples with the same set of MHKS parameters, as is usually carried out with non-branched polymers. A very similar result is—not surprisingly—obtained for poly(MA). Only the plot determined on the sample generated at 60 °C does not overlap with the other data. For the 60 °C data set a significantly different pair of MHKS values are obtained when the traces are fitted individually (from the 60 °C data alone, $\alpha = 0.54$ is deduced)

As no trend with increasing temperature for the individual samples is observed, it can be assumed with reasonable confidence that the 60 °C data point represent an outlier. Thus, analogues to polyEHA, a joint fit of all traces has been carried out without taking the 60 °C data set into account. The resulting K and α from the joint fits are provided in Table 2. The poly(MA) parameters were thus determined from PLP samples prepared in bulk in the temperature range between 20 and 85 °C, with a molecular weight range of 1.6×10^4 to $2 \times 10^5 \text{ g} \cdot \text{mol}^{-1}$. The poly(2-EHA) parameters were determined predominantly from samples made under PLP conditions in bulk, yet including a few samples in solution (toluene) in the temperature range between 15 and 80 °C, with a molecular weight range of 6500 to $6 \times 10^6 \text{ g} \cdot \text{mol}^{-1}$.

Determination of Propagation Rate Coefficients over a Wide Temperature Range for Methyl Acrylate and 2-Ethylhexyl Acrylate. With these data at hand, one can now proceed to analyze the PLP samples for their characteristic

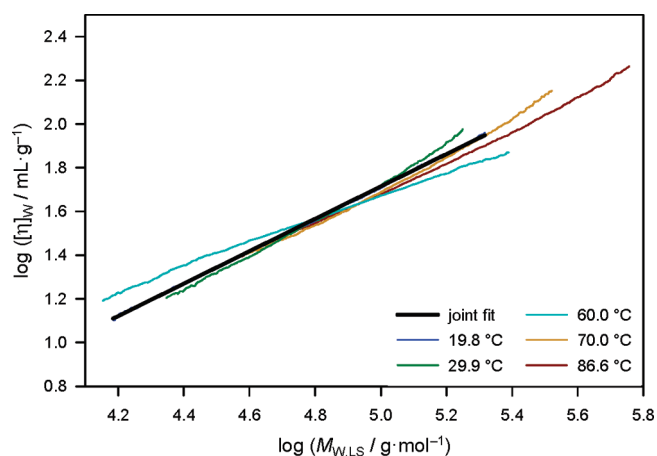


Figure 4. Linear regions of intrinsic viscosity for poly(MA) from which MHKS parameters were determined. The linear black line represents the best fit of all data presented in the figure. The conditions under which poly(MA) samples were generated are found in the legend.

Table 2. Global MHKS Parameters for Poly(MA) and polyEHA As Determined from Samples Prepared at Temperatures Ranging from 20 to 80 °C

polymer	$K \times 10^5 / \text{dL} \cdot \text{g}^{-1}$	α
poly(MA)	10.2	0.741
polyEHA	9.85	0.719

peak patterns and molecular weights via conventional SEC. The detailed procedure and the theory behind PLP can be found elsewhere,^{6–8,24} thus only a short summary of the principle behind PLP is provided here. By the incidence of each laser pulse, initiator-derived radicals are formed which subsequently start chain growth in the dark-time period. As no initiation takes place in the time after a pulse was applied, a close-to monodisperse growth of macroradicals can be assumed and hence the length of a radical be correlated with the time after the laser pulse. With each subsequent laser pulse, not only are new radicals generated, but also most of the growing chains are terminated. A few radicals may however survive and grow for multiple dark time periods. The resulting molecular weight distribution is complex and multimodal, yet characteristic for PLP. For the evaluation of propagation rate coefficients from these distributions, it is sufficient to state that k_p is always determined from the molecular weight at the first inflection point (or in principle from any higher inflection points) of the multimodal molecular weight distribution. The propagation rate coefficient, k_p is thus readily deduced via:

$$L_i = k_p \cdot c_M \cdot i \cdot t_0, \quad \text{where } i = 1, 2, 3, \dots \quad (1)$$

where L is the degree of polymerization at the inflection points, c_M is the monomer concentration and t_0 is the darktime between two consecutive laser pulses. A collation of the molecular weight distributions and their first derivatives used for the determination of the inflection points of all PLP samples are given in the Supporting Information. All relevant information derived from these plots for the monomer MA are given in Table 3.

Monomer concentrations are calculated from the monomer density $\rho(T)$ (see Supporting Information for further details). The resulting k_p from the first point of inflection is provided in Table 2. Additionally, the ratio of the propagation rate coefficient determined from the first inflection point over the propagation rate determined from the second point of inflection is listed. This ratio can serve as a quality measure for the experiment as in principle $k_{p,1}$ and $k_{p,2}$ should be identical. Deviations between 5 and 25% are however commonly seen.^{22,24–27} This is often observed with acrylate monomers and can be attributed to the occurrence of MCRs.¹⁴ MCRs decrease the average propagation rate due to their significantly lower reactivity. It should be noted that such a decrease in the average propagation rate allows in principle for the determination of the midchain radical specific rate coefficients, which was however not the scope of the present

Table 3. Evaluated Data for the Determination of k_p for MA^a

$T/^\circ\text{C}$	n	$c_M / \text{mol} \cdot \text{L}^{-1}$	$\log(M_1 / \text{g} \cdot \text{mol}^{-1})$	$\log(M_2 / \text{g} \cdot \text{mol}^{-1})$	$k_{p,1} / \text{L} \cdot \text{mol}^{-1} \cdot \text{s}^{-1}$	$k_{p,1}/k_{p,2}$
11.3	60	11.20	4.258	4.509	9401	1.12
11.9	100	11.19	4.298	4.553	10320	1.11
19.8	600	11.08	4.395	4.674	13011	1.05
20.4	100	11.07	4.388	4.665	12826	1.06
29.7	500	10.94	4.475	4.735	15851	1.10
30.8	100	10.93	4.419	4.678	13944	1.10
40.3	200	10.80	4.593	4.847	21079	1.11
40.3	250	10.80	4.601	4.851	21480	1.12
50.2	200	10.66	4.679	4.906	26041	1.19
50.4	250	10.66	4.683	4.911	26297	1.19
60.5	200	10.53	4.758	4.962	31654	1.25
60.6	150	10.52	4.763	4.971	31965	1.24
70.9	150	10.39	4.800	5.005	35328	1.25
71.0	100	10.39	4.800	4.996	35332	1.27
81.2	100	10.26	4.767	5.022	33123	1.11
81.2	200	10.26	4.767		33123	

^a n gives the number of pulses applied during the experiment and M_i represents the respective molecular weights at the inflection points.

study. Such a retardation effect, while also present in the first dark-time period between two consecutive laser pulses, has more severe effects on the second inflection points compared to the first due to the fact that the radicals had twice as much time to undergo a transfer step. The data from Table 3 is depicted in Figure 5 in the form of an Arrhenius plot. A good linearity of the data is seen between 10 and 60 °C. For the higher temperatures ($T > 70$ °C), k_p levels off and does not fit the Arrhenius behavior anymore. Such an observation, accompanied by a concomitant loss of a second inflection point at 80 °C, is commonly observed for other acrylates (including *n*-butyl acrylate) under the same reaction conditions.^{22,24,25} Further indicated in the plot are error margins for each data point. The analysis of the local dispersities for each temperature suggests that the relative error of k_p should be constant over the studied temperature regime, being close to 20%, based on the molecular weight analysis error induced by the local dispersity level of 1.2 (see above and Figure 2). To account for additional errors inherent to the PLP-SEC experiment, an overall error margin of 30% was assumed for all samples (resulting in $\pm 15\%$ error limits). For the fitting of the data, a nonlinear least-squares method as implemented in the software Contour 2.02 by van Herk was employed.⁴⁴ For the weighting of the error, a normal distribution was assumed. Such an assumption may not be entirely justified as the potentially

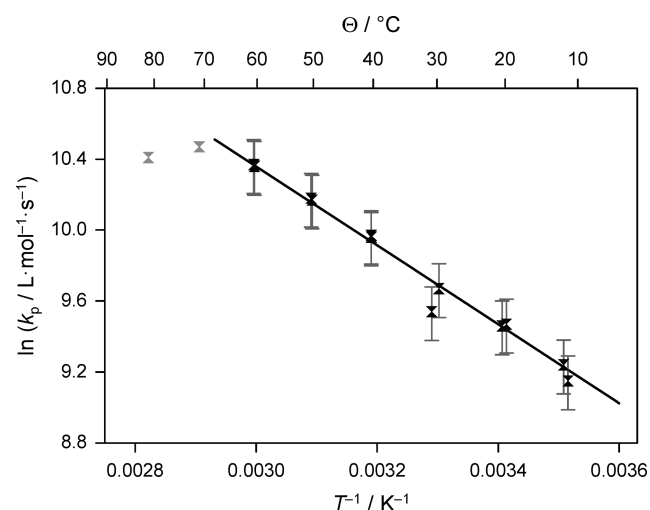


Figure 5. Arrhenius plot for the propagation rate coefficient of MA based on the data given in Table 3.

erroneous determination of molecular weights is not statistical, yet such data treatment seems to be justifiable. A minimum in the sum of squares space (straight line in Figure 5) is found for the activation energy $E_A = 18.5$ ($+0.8$ to -0.9) $\text{kJ}\cdot\text{mol}^{-1}$ and the frequency factor $A = 2.5$ ($+1.2$ to -0.6) $\times 10^7 \text{ L}\cdot\text{mol}^{-1}\cdot\text{s}^{-1}$ in the temperature range between 10 and 60 °C. Even though relatively large errors were assumed for the molecular weight characterization, the residual error is relatively small with approximately $\pm 1 \text{ kJ}\cdot\text{mol}^{-1}$, in the range of errors found in previous studies on acrylate systems.^{22,24,25}

The propagation rate coefficient of MA has been previously targeted in PLP experiments and with 100 Hz lasers, data for low temperatures were obtained. Manders⁴⁵ obtained an activation energy of $17.7 \text{ kJ}\cdot\text{mol}^{-1}$ with an associated frequency factor of $1.7 \times 10^7 \text{ L}\cdot\text{mol}^{-1}\cdot\text{s}^{-1}$. In the same laboratories, Willemse et al. arrived at an activation energy of $18.3 \text{ kJ}\cdot\text{mol}^{-1}$ and $A = 2.4 \times 10^7 \text{ L}\cdot\text{mol}^{-1}\cdot\text{s}^{-1}$.⁴⁶ In addition, Buback and co-workers have studied the low-temperature propagation rate coefficient of methyl acrylate via PLP-SEC.⁴⁷ These authors, however, studied the influence of pressure on k_p , and only limited temperature dependent data was obtained thus disallow for a determination of activation energy and pre-exponential factor. From the studies available in literature, the value from Willemse et al. is not affected by branching of the samples as it was determined on the basis of molecular weight determinations via MALDI-ToF mass spectrometry and thus appears to be more reliable.⁴³ However, due to the limitation of the applied repetition rate, only the temperature range of -25 to $+8$ °C could be studied. A commencing influence of backbiting even at these low temperatures cannot be excluded due to the comparatively low laser repetition rate of 100 Hz. Thus, even though the experimental error in the temperature range was assumed to be very low, an increased error could not have been excluded for the extrapolation to the temperature range that was covered in the current study. Similar to *n*-butyl acrylate,²² however, the low-temperature data obtained from 100 Hz experiments are in excellent agreement with the results from the present study.

The resulting k_p data for polyEHA are collated in Table 4 and plotted in Figure 6. Monomer concentrations were again calculated on the basis of literature reported temperature dependent density data $\rho(T)$ (see Supporting Information for further details).⁴⁸ A similar behavior of the propagation rate coefficient as for MA can be observed: up to 60 °C a good linearity of the Arrhenius plot is observed with deviations for the data points obtained at 70 and 80 °C. The agreement between the resulting k_p from the first two inflection points is

Table 4. Evaluated Data for the Determination of k_p for EHA^a

$T/\text{°C}$	n	$c_M/\text{mol}\cdot\text{L}^{-1}$	$\log(M_1/\text{g}\cdot\text{mol}^{-1})$	$\log(M_2/\text{g}\cdot\text{mol}^{-1})$	$k_{p,1}/\text{L}\cdot\text{mol}^{-1}\cdot\text{s}^{-1}$	$k_{p,1}/k_{p,2}$
10.1	850	4.85	4.271	4.563	10 440	1.02
10.2	850	4.85	4.313	4.561	11 500	1.13
20	750	4.80	4.409	4.775	14 490	0.86
20.7	750	4.80	4.425	4.774	15 050	0.89
29.7	600	4.76	4.481	4.779	17 280	1.01
29.8	600	4.76	4.504	4.791	18 190	1.03
40.8	500	4.71	4.578	4.838	21 820	1.10
40.9	500	4.71	4.573	4.833	21 550	1.10
50.8	450	4.67	4.652		26 090	
50.8	450	4.67	4.606		23 470	
60.8	350	4.62	4.721		30 860	
60.9	350	4.62	4.751		33 060	
71.2	350	4.58	4.725		31 450	
71.2	350	4.58	4.800		37 400	
81.2	300	4.54	4.758		34 250	
81.5	300	4.53	4.825		39 990	

^a n gives the number of pulses applied during the experiment and M_i represents the respective molecular weights at the inflection points.

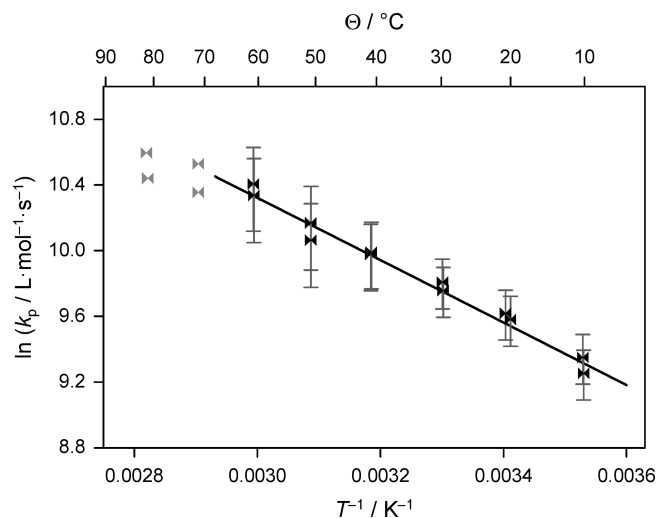


Figure 6. Arrhenius plot for the propagation rate coefficient of EHA based on the data given in Table 4.

slightly better for 2-ethylhexyl acrylate, however, no second point of inflection was observable from as low as 50 °C on. Such a finding indicates that more transfer events occur compared to the other monomers, leading to a blurring of the molecular weight distribution at even lower temperatures (from 50 °C onward). The hypothesis that during EHA polymerization more transfer events occur leading to an increased level of (long)-chain branches is underpinned by the higher local dispersity values seen for this monomer (see Figure 2 above, where the local dispersity exceeds 1.5 from 50 °C onward). Thus, the disappearance of the second inflection point is not necessarily a consequence of the retarding action of the midchain radicals and—consequently—the data between 50 and 60 °C can be used to derive an activation energy. It should, however, be noted that fitting the data only in the range up to 50 °C would yield a slightly larger activation energy. This increase is not significant within the scatter of the data.

For the fitting of the data to an Arrhenius equation, an identical procedure as for MA was applied. The difference with the EHA data is, however, that in this case no even distribution of the relative errors can be assumed. Again, a minimum error of 30% was assumed, however for all samples where average $D(V_c)$ above 1.3 were identified, the error was calculated based on each individual local dispersity value as outlined above, leading to 50% error margins at 60 °C. The resulting Arrhenius parameters are thus beset with a considerably larger error and read $E_A = 15.8 (+1.6 \text{ to } -1.4) \text{ kJ} \cdot \text{mol}^{-1}$ and $A = 9.1 (+10.1 \text{ to } -2.9) \times 10^6 \text{ L} \cdot \text{mol}^{-1} \cdot \text{s}^{-1}$ for the temperature range up to 60 °C. The scatter of the data between MA and EHA k_p is comparable. Thus, the increased error in the activation energy can be attributed to the decreased accuracy of the SEC analysis. Castignolles determined the temperature dependence of EHA k_p with $E_A = 16.9 \text{ kJ} \cdot \text{mol}^{-1}$ and a frequency factor of $A = 13.1 \times 10^6 \text{ L} \cdot \text{mol}^{-1} \cdot \text{s}^{-1}$ in the temperature range of $-35 \text{ °C} \leq T \leq 25 \text{ °C}$ (including reinjection of samples).^{48,49} Hutchinson and co-workers determined some propagation rate coefficients, yet in the range $5 \text{ °C} \leq T \leq 25 \text{ °C}$ and did not determine the activation energy in such a narrow temperature range.⁵⁰ Taking the higher relative error into account, a gratifying generally good agreement with the existing literature data is observed, however with data derived from a significantly larger temperature range.

The identified activation energy of EHA is significantly below the one found for MA and also lower than for other

alkyl acrylates.^{22,24} However—also for the corresponding methacrylates—a decrease in E_A by close to $2\text{--}2.5 \text{ kJ} \cdot \text{mol}^{-1}$ is observed when going from the methyl and the butyl ester to 2-ethylhexyl methacrylate.^{4,51} A physical explanation for this reduction cannot readily be provided, yet the manifest assumption of the bulky, yet flexible ester side chain having an influence on the dynamics of the growing macroradicals appears to be reasonable.

Conclusions

The determination of free radical polymerization propagation rate coefficients, k_p , for acrylates can be complicated by side reactions that secondary propagating radicals undergo, which typically involves the formation of midchain radicals. On the one hand, these side reactions can lead to a blurring of the molecular weight distribution during the PLP experiments—particularly at elevated temperatures—invalidate the chain length–time correlation. These effects can to some degree be compensated by employing high repetition rate lasers (i.e., 500 Hz) as in the present study. On the other hand, the long and short chain branches which are generated during the polymerization process can severely complicate the SEC analysis of the PLP samples. In the current contribution, we have thus subjected polymers prepared in a wide temperature range (from 20 to 80 °C) to a procedure which allowed for the estimation of their so-called local dispersity, $D(V_c)$, in order to get an indication of the local inhomogeneities of the polymeric materials and thus a measure for the potential SEC error when using a conventional calibration. The local dispersity value represents a measure for the degree of branching in a polymer samples. Interestingly, poly(MA) samples displayed—as a function of temperature—considerably lower dispersities than samples of polyEHA. The obtained local dispersity values allowed for an estimation of the SEC error, which would ultimately beset the derived Arrhenius parameters of the propagation rate coefficient. The potentially higher branching level in EHA—caused by a more pronounced transfer activity—also manifested itself in less structured molecular weight distributions for polyEHA at elevated temperatures (from 50 °C onward). The key information on the present study is thus centered on the estimation—to the best of our knowledge for the first time—of errors in the PLP–SEC of acrylates caused by the SEC analysis as well as the provision of Arrhenius parameters of k_p for MA and EHA for temperatures of up to 70 °C. The obtained activation energies and pre-exponential factors are in good agreement with previous data obtained in a more limited temperature range up to 20 °C employing 100 Hz lasers. As error besetting k_p exhibits a strong systematic component, the estimate of the error will in future allow for more meaningful studies into the variation of k_p with the alkyl side chain group within the acrylate family.

Acknowledgment. C.B.-K. acknowledges the Karlsruhe Institute of Technology (KIT) within the context of the *Excellence Initiative* for leading German Universities for supporting the current project.

Supporting Information Available: Figures showing all recorded PLP–SEC traces and their first derivatives for the determination of the inflection points, the plots from which the local dispersities were derived as well as tables and figures showing the density at different temperatures for the monomers. This material is available free of charge via the Internet at <http://pubs.acs.org>.

References and Notes

- Matyjaszewski, K.; Xia, J. *Chem. Rev.* **2001**, *101*, 2921.
- Chieffari, J.; Jeffery, J.; Mayadunne, R. T. A.; Moad, G.; Rizzardo, E.; Thang, S. H. *Macromolecules* **1999**, *32*, 7700–7704.

- (3) Hawker, C. J.; Bosman, A. W.; Harth, E. *Chem. Rev.* **2001**, *301*, 3661.
- (4) Beuermann, S.; Buback, M. *Prog. Polym. Sci.* **2002**, *27*, 191–254.
- (5) Barner-Kowollik, C.; Buback, M.; Egorov, M.; Fukuda, T.; Goto, A.; Russell, G. T.; Vana, P.; Yamada, B.; Zetterlund, P. B. *Prog. Polym. Sci.* **2005**, *30*, 605.
- (6) Olaj, O. F.; Bitai, I.; Hinkelmann, F. *Makromol. Chem.* **1987**, *188*, 1689–1702.
- (7) Buback, M.; Gilbert, R. G.; Hutchinson, R. A.; Klumpermann, B.; Kuchta, F. D.; O'Driscoll, K. F.; Russell, G. T.; Schweer, J. *Macromol. Chem. Phys.* **1995**, *196*, 3267.
- (8) For an example, see: Asua, J. M.; Beuermann, S.; Buback, M.; Castignolles, P.; Charleux, B.; Gilbert, R. G.; Hutchinson, R. A.; Leiza, J. R.; Nikitin, A. N.; Vairon, J.-P.; van Herk, A. M. *Macromol. Chem. Phys.* **2004**, *205*, 2151.
- (9) Plessis, C.; Arzamendi, G.; Alberdi, J. M.; van Herk, A. M.; Leiza, J. R.; Asua, J. M. *Macromol. Rapid Commun.* **2003**, *24*, 173–177.
- (10) Willemse, R. X. E.; van Herk, A. M.; Panchenko, E.; Junkers, T.; Buback, M. *Macromolecules* **2005**, *38*, 5098–5103.
- (11) Buback, M.; Hesse, P.; Junkers, T.; Sergeeva, T.; Theis, T. *Macromolecules* **2008**, *41*, 288–291.
- (12) Barth, J.; Buback, M.; Hesse, P.; Sergeeva, T. *Macromol. Rapid Commun.* **2009**, *30*, 1969–1974.
- (13) Nikitin, A. N.; Castignolles, P.; Charleux, B.; Vairon, J.-P. *Macromol. Rapid Commun.* **2003**, *24*, 778–782.
- (14) Junkers, T.; Barner-Kowollik, C. *J. Polym. Sci., Polym. Chem.* **2008**, *46*, 7585–7605.
- (15) Hamielec, A. E.; Ouano, A. C.; Nebenzahl, L. L. *J. Liq. Chrom.* **1978**, *1* (4), 527–554.
- (16) Hamielec, A. E.; Ouano, A. C. *J. Liq. Chrom.* **1978**, *1* (1), 111–120.
- (17) Kostanski, L. K.; Keller, D. M.; Hamielec, A. E. *J. Biochem. Biophys. Methods* **2004**, *58* (2), 159–186.
- (18) Gaborieau, M.; Gilbert, R. G.; Gray-Weale, A.; Hernandez, J. M.; Castignolles, P. *Macromol. Theory Simul.* **2007**, *16*, 13–28.
- (19) Gaborieau, M.; Nicolas, J.; Save, M.; Charleux, B.; Vairon, J.-P.; Gilbert, R. G.; Castignolles, P. *J. Chromatogr. A* **2008**, *1190*, 215–233.
- (20) Castignolles, P.; Graf, R.; Parkinson, M.; Wilhelm, M.; Gaborieau, M. *Polymer* **2009**, *50*, 2372–2383.
- (21) Castignolles, P. *Macromol. Rapid Commun.* **2009**, *30*, 1995–2001.
- (22) Barner-Kowollik, C.; Günzler, F.; Junkers, T. *Macromolecules* **2008**, *41* (23), 8971–8973.
- (23) van Herk, A. M. *Macromol. Rapid Commun.* **2001**, *22*, 687–689.
- (24) Dervaux, B.; Junkers, T.; Schneider-Baumann, M.; Du Prez, F. E.; Barner-Kowollik, C. *J. Polym. Sci.—Polym. Chem.* **2009**, *47*, 6641–6654.
- (25) Barner-Kowollik, C.; Bennet, F.; Schneider-Baumann, M.; Voll, D.; Rölle, T.; Fäcke, T.; Weiser, M.-S.; Bruder, F.-K.; Junkers, T. *Polym. Chem.* **2010**, *1*, 470–479.
- (26) Junkers, T.; Koo, S. P. S.; Barner-Kowollik, C. *Polym. Chem.* **2010**, *1*, 438–441.
- (27) Junkers, T.; Voll, D.; Barner-Kowollik, C. *e-Polym.* **2009**, 076.
- (28) Strazielle, C.; Benoit, H.; Vogl, O. *Eur. Polym. J.* **1978**, *14*, 331–334.
- (29) Rudin, A.; Hoegy, H. L. W. *J. Polym. Sci., A-1* **1972**, *10*, 217.
- (30) Penzel, E.; Goetz, N. *Angew. Makromol. Chem.* **1990**, *178*, 191–200.
- (31) Lathová, E.; Lath, D.; Pavlinec, J. *Polym. Bull.* **1993**, *30*, 713–718.
- (32) Striegel, A. M.; Kirkland, J. J.; Yau, W. W.; Bly, D. D. *Modern Size Exclusion Chromatography*, 2nd ed.; Wiley: Hoboken, NJ, 2009; pp 248–249.
- (33) Ahmad, N. M.; Heatley, F.; Lovell, P. A. *Macromolecules* **1998**, *31*, 2822–2827.
- (34) Gaborieau, M.; Koo, S. P. S.; Castignolles, P.; Junkers, T.; Barner-Kowollik, C. *Macromolecules* **2010**, *43*, 5492–5495.
- (35) Nikitin, A. N.; Hutchinson, R. A.; Buback, M.; Hesse, P. *Macromolecules* **2007**, *40*, 8631–8641.
- (36) Tackx, P.; Bosscher, F. *Anal. Commun.* **1997**, *34* (10), 295–297.
- (37) Junkers, T. Ph.D. thesis, Georg August Universität Göttingen: Göttingen, Germany, 2006.
- (38) Ahmad, N. M.; Heatley, F.; Lovell, P. A. *Macromolecules* **1998**, *31*, 2822–2827.
- (39) Heatley, F.; Lovell, P. A.; Yamashita, T. *Macromolecules* **2001**, *34*, 7636–7641.
- (40) Junkers, T.; Bennet, F.; Koo, S. P. S.; Barner-Kowollik, C. *J. Polym. Sci.—Polym. Chem.* **2008**, *46*, 3433–3437.
- (41) Zorn, A. M.; Junkers, T.; Barner-Kowollik, C. *Macromol. Rapid Commun.* **2009**, *30*, 2028–2035.
- (42) Schmitt, B. Ph.D. thesis, University of Mainz: Mainz, Germany, 1999.
- (43) Mrkvickova, L.; Danhelka, J.; Vlcek, P. *Polym. Commun.* **1990**, *31* (11), 416–417.
- (44) van Herk, A. M.; Dröge, T. *Macromol. Theory Simul.* **1997**, *6*, 1263.
- (45) Manders, B. G. Ph.D. thesis, Eindhoven University of Technology: Eindhoven, The Netherlands, 1997.
- (46) Willemse, R. X. E.; van Herk, A. M. *Macromol. Chem. Phys.* **2010**, *211*, 539–545.
- (47) Buback, M.; Kurz, C. H.; Schmaltz, C. *Macromol. Chem. Phys.* **1998**, *199*, 1721–1727.
- (48) Couvreur, L.; Piteau, G.; Castignolles, P.; Tonge, M.; Coutin, B.; Charleux, B.; Vairon, J.-P. *Macromol. Symp.* **2001**, *174*, 197–208.
- (49) Castignolles, P. Ph.D. thesis, University Pierre and Marie Curie: Paris, 2003.
- (50) Beuermann, S.; Paquet, D. A.; McMin, J. H.; Hutchinson, R. A. *Macromolecules* **1996**, *29*, 4206–4215.
- (51) Hutchinson, R. A.; Beuermann, S.; Paquet, D. A.; McMin, J. H. *Macromolecules* **1997**, *30*, 3490.